



Trade Science Inc.

Nano Science and Nano Technology

An Indian Journal

Full Paper

NSNTAJ, 6(1), 2012 [1-4]

Efficiency enhancement of solar cells by nanoscale morphology

P.Dileep^{1*}, K.R.Shankarkumar²¹Anna University of Technology, Coimbatore, (INDIA)²Sri Ramakrishna Engineering College, Coimbatore (INDIA)

E-mail : dileep@hotmail.com

Received: 12th December, 2011 ; Accepted: 18th January, 2012

ABSTRACT

The Nanoscale morphology has been shown to be a critical parameter governing charge transport properties of polymer bulk heterojunction (BHJ) solar cells. Recent results on vertical phase separation have intensified the research on 3D morphology control. In this paper, we intend to modify the distribution of donors and acceptors in a classical BHJ polymer solar cell by making the active layer richer in donors and acceptors near the anode and cathode respectively. Here, we chose [6,6]-phenyl-C61-butyric acid methyl ester (PCBM) to be the acceptor material to be thermally deposited on top of [poly(3-hexylthiophene)] P3HT: the PCBM active layer to achieve a vertical composition gradient in the BHJ structure. Here we report on a solar cell with enhanced power conversion efficiency of 4.5% which can be directly correlated with the decrease in series resistance of the device.

© 2012 Trade Science Inc. - INDIA

KEYWORDS

P3HT:PCBM;
Morphology;
Bulk hetero junction;
Nanoscale;
Annealing;
Organic solar cells.

INTRODUCTION

Organic Photovoltaics have generated significant interest because of their several inherent advantages over other forms of solar cells. They offer a cheap, light-weight and flexible technology to harvest sun's energy. A remarkable improvement in the device performance has been achieved since photo-induced electron transfer from conjugated polymer to fullerene was first reported in 1992^[1]. The most important breakthrough on which most of today's device structures are based was the introduction of bulk heterojunction (BHJ)^[2] wherein the p-type (donor) and the n-type (acceptor) materials are blended together in the film to create an interpenetrating network at a nanoscale and hence a large surface area for donor-

acceptor interface.

The device morphology plays a critical role in the power conversion efficiency of organic solar cells. Thermal annealing, solvent annealing^[3, 4] and greater regioregularity^[5] have shown to improve the morphology of polymers to enhance charge transport and minimize charge recombination. This nanoscale morphology in turn controls the exciton diffusion and charge transport properties. It is agreed that the optimum nanoscale morphology must be a balance between a large interfacial area and continuous pathways for carrier transportation^[6]. The recent researches shown the evidence of the nanoscale phase segregation in vertical direction (perpendicular to the electrodes) for the poly(3-hexylthiophene): [6,6]-phenyl-C61-butyric acid methyl ester (P3HT-PCBM) blends and its dependence

Full Paper

on several processing parameters. Now, it is pretty clear that the spin-cast film is not exactly a uniform blend of donor and acceptor.



Figure 1 : A bulk heterojunction with composition gradient: spin coated polymer BHJ sandwiched between the acceptor rich and donor rich layers near the cathode and anode respectively, for an ideal solar cell.

The structure for solar cell would be one where the active layer is sandwiched between a donor (p-type) rich layer near the high work function anode and an acceptor (n-type) rich layer near the low work function cathode (Figure 1) to maximize charge extraction efficiency. But this in fact is not true. We recently reported that the ‘solvent annealed’ P3HT:PCBM film has significantly higher P3HT (donor) on the top of the film^[8]. To correct this, in this paper, we want to artificially achieve a polymer layer, with a vertically graded distribution of the BHJ composition. This unique approach to modulate the distribution of donor–acceptor at such a nanoscale in the spin coated layer is similar to the p–i–n-type solar cells for inorganic devices or small molecule (organic) solar cells. However, this kind of control for spin coated layers has proven to be difficult. Here, we achieve enhanced power conversion efficiency (PCE) by demonstrating the vertically graded distribution in BHJ structure for spin coated films.

The interface problems or energy losses for transport of free electrons to the cathode are minimized in these structures. This will also reduce recombination losses at contacts. This work is fundamentally unique from previous approaches of using a low LUMO level/work function material between the active layer and the cathode^[9, 10] because here we modify the gradient in the BHJ rather than add a separate material to improve charge extraction at the cathodes.

In our research we choose PCBM to be the acceptor material (pure n) to be thermally evaporated between the BHJ and the cathode. The thickness of this acceptor layer can be easily modulated to opti-

mize the position of active layer with respect to the maxima of the optical field distribution. Playing an essential role in charge transport near the cathode, it provides an ohmic contact for electrons for transport between the BHJ and PCBM. But there is a Schottky barrier for the injection of photo-generated holes into PCBM as minority carriers. In this way, the PCBM rich top interface acts as a ‘filter’ allowing only the ‘right’ type of charge carriers (electrons) to leave the photoactive layer.

EXPERIMENTAL DETAILS

We choose the device structure of ITO/poly(3,4-ethylenedioxythiophene) poly (styrenesulfonate) (PEDOT:PSS) / P3HT:PCBM (1:1 ratio)/PCBM/Ca/Al (device A). The reference device for all the experiments had the structure ITO/PEDOT:PSS/P3HT:PCBM/Ca/Al (device B). For device fabrication, PEDOT:PSS was spin coated (and annealed at 130 °C for 20 min) on pre-cleaned and 15 min UV–ozone-treated ITO glass substrates. RR-P3HT and PCBM were separately dissolved in 1,2- dichlorobenzene, then blended together with 1:1 wt/wt ratio to form a 2 wt% solution. This RR-P3HT/PCBM solution was spin coated at 700 rpm for 40 s, and the wet film was dried in a covered glass Petri dish as in^[4]. The dried film was then annealed at 110 °C for 10 min. The active film thickness was 210 to 230 nm measured by a Dektak 3030 profilometer. The cathode was 20 nm Ca and 80 nm Al. For device A, different thickness of PCBM was thermally evaporated on top of the BHJ active layer at a rate of 0.2–0.3 Å s⁻¹ at a pressure of 2×10^{-6} Torr.

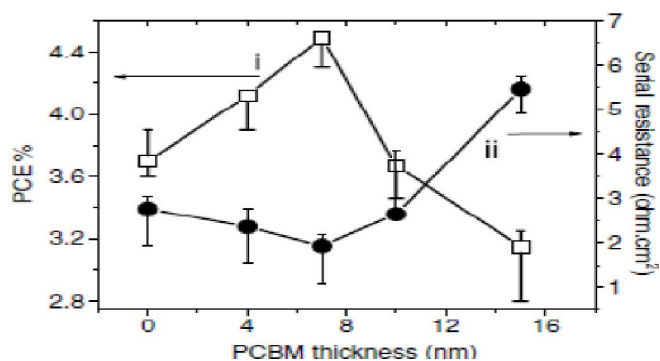


Figure 2 : Effect of PCBM thickness on device performance: plot shows power conversion efficiency (open squares, curve i) and series resistance (fill circles, curve ii) for different thicknesses of PCBM layer annealed at 110 °C for 30 min in device A. Device area was 0.12 cm².

A second annealing step in the glove box (N₂ atmosphere) is performed after the deposition of the PCBM layer. The devices were tested in the glove box under simulated AM1.5G irradiation (with an intensity of 100 mW cm⁻²) by using a solar simulator. The illumination intensity was determined by a NREL calibrated Si detector with KG-5 color filter, and the spectral mismatch was corrected^[11].

RESULTS AND DISCUSSION

The PCE data (curve I) for device A corresponding to different thicknesses of PCBM layer annealed at 110 °C for 30 min. are shown in Figure 2. It shows a maximum in efficiency value (approximately 4.5%) at 7 nm PCBM thickness corresponding to a minimum in the series resistance of these devices (curve II in Figure 2). The series resistance was derived from the slope of the *J-V* characteristic curve under dark close to 2 V. Although the transport of electron through PCBM is not energetically unfavorable but still there should be an increased series resistance on increasing the PCBM thickness.

A possible explanation is that as the coverage of PCBM increases, the charge collection efficiency at the cathode increases due to availability of better conduction paths for the electrons. This offsets the possible increase in series resistance until a point where the PCBM coverage is almost complete. After this transition point seen at 7 nm of PCBM, the coverage is more or less complete and deposition of any more PCBM leads to an increase in series resistance value as should be expected. Prior works on annealing of P3HT:PCBM devices have shown to increase its PCE significantly^[12].

The Annealing has shown to enable nanocrystallization, diffusion of the components in the blend^[12-14] and improve the nanoscale morphology which can strongly affect the transport pathways for free charges^[3, 15]. Device A with different thickness of PCBM on BHJ, all show improved performance on annealing for just 10 min at 110 °C. For all thicknesses of deposited PCBM, when the top PCBM layer is not annealed it shows a fall in efficiency due to a decrease in fill factor. We suspected that the improvement in device efficiency with annealing time to be related to the top PCBM layer. To understand the effects of thermal annealing, morphological studies were done using

atomic force microscopy (AFM) as shown in Figure 3. PCBM has been shown to have a high tendency to crystallize^[16].

Hence, we expected that the reason for improved performance after annealing was related to crystallization of the top 7 nm of PCBM layer and the resulting improvement in charge transport.

Height images of the unannealed (Figure 3(a)) and

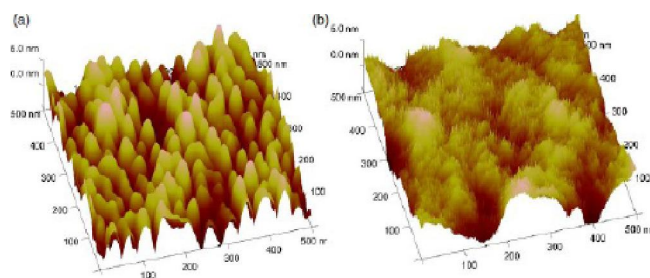


Figure 3 : Effect of annealing on morphology of top PCBM layer: AFM height images of device A showing a 500 nm × 500 nm surface area. (a) Unannealed 7 nm PCBM layer; (b) 7 nm PCBM layer annealed at 110 °C for 30 min. Scale on z axis = 5 nm.

annealed (Figure 3(b)) devices showed that the unannealed layer had a mean square root roughness of 2.05 nm which reduced to 1.28 nm on annealing. Hence, PCBM layer smoothes the top surface since it has been shown that the P3HT:PCBM layer has a roughness of 9.5 nm^[4]. Figure 3(a) of the unannealed device shows large mounds and valleys of approximately 20 nm width on the surface. On annealing, these smoothed out giving a nanotexture to the film with feature sizes within a couple of nanometer width.

This resulted in smoother films but with a higher effective area of contact between the cathode and the electron transporting PCBM layer, which lead to better electron transport characteristics.

This can be explained by the following scenario: after deposition of PCBM on a BHJ layer, we in fact have a PCBM layer on top of the BHJ with a sharp BHJ/PCBM interface which is not preferred for the device.

When we anneal at extended time, the sharp interface disappears with diffusion of PCBM into the BHJ introduced by thermal energy, making the top few nanometers of the BHJ rich in PCBM (acceptor) which helps device performance. This can be directly related to the decrease in series resistance that we observe on the macroscopic scale from the current–voltage (*J-V*) characteristics, as shown in Figure 4.

Full Paper

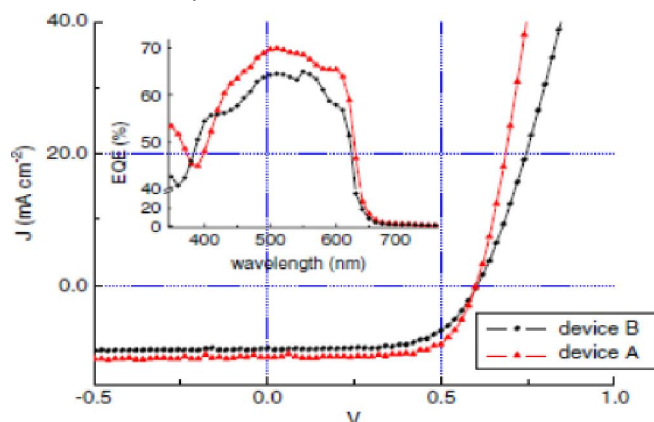


Figure 4 : Effect of donor layer (PCBM) on performance of polymer solar cells: current–voltage ($J-V$) characteristics of reference device B (black circle) with the structure ITO/PEDOT-PSS/P3HT:PCBM/Ca/Al and for device A (red up-triangle) with the structure ITO/PEDOT-PSS/P3HT:PCBM/Ca/Al. Inset shows the EQE measurements for device A and reference device B.

An optimized device A shown in Figure 4 which was annealed at 110 °C for 30 min showing an improvement in PCE as compared to reference device B from 3.8% to 4.5%. There is an increase in J_{sc} from 9.52 mA cm⁻² for the reference device B to 10.92 mA cm⁻² for the device A. This increase in J_{sc} is mainly attributed to the decrease in series resistance from 2.06 Ω cm² for device B to 1.33 Ω cm² for device A. The PCBM rich top layer increases the electron collection efficiency of the cathodes. The decrease in series resistance is attributed to better conduction path available to the electrons between the BHJ and the cathode. The inset of Figure 4 shows that the EQE maximum for the device A is 70% while that for reference device B was approximately 64%. The integral of the product of this absolute EQE and the global reference spectrum yields a J_{sc} of 9.2 mAcm⁻² for device B and 10.2 mAcm⁻² for device A, which matches closely to the EQE measured for these individual devices.

There is a uniform increase in EQE for device A as compared to B in almost the entire wavelength range. This is consistent with our reasoning that PCBM on top of the P3HT:PCBM active layer forms a better interface leading to better charge extraction. To check reproducibility, multiple batches with the same conditions as reported above were made. The average device efficiency was 4.4%. This is an increase of approximately 15% over reference devices.

CONCLUSIONS

The studied device architecture shows an increased efficiency. The spin coated BHJ structure with graded composition increases the efficiency. This increase in efficiency due to improved transport and extraction of electrons near the cathode. The thermal annealing step increases the PCBM concentration in the top few nanometer of the active layer due to PCBM diffusion and hence this improved vertical morphology contributes to the increase in efficiency. The BHJ architecture for spin coated films have a P3HT rich zone between the BHJ and the anode will shows further improvement in efficiency.

REFERENCES

- [1] N.S.Sariciftci, L.Smilowitz, A.J.Heeger, F.Wudl; *Science*, **258**, 1474 (1992).
- [2] G.Yu, A.J.Heeger; *J.Appl.Phys.*, **78**, 4510 (1995).
- [3] G.Li, V.Shrotriya, J.Huang, Y.Yao, T.Moriarty, K.Emery, Y.Yang; *Nat.Mater.*, **4**, 864 (2005).
- [4] G.Li, Y.Yao, H.Yang, V.Shrotriya, G.Yang, Y.Yang; *Adv.Funct.Mater.*, **17**, 1636 (2007).
- [5] Y.Kim et al.; *Nat.Mater.*, **5**, 197 (2006).
- [6] H.Hoppe, N.S.Sariciftci; *J.Mater.Chem.*, **16**, 45 (2006).
- [7] M.C.Quiles, T.Ferenczi, T.Agostinelli, P.Etchegoin, Y.Kim, T.Anthopoulos, P.Stavrinou, D.Bradley, J.Nelson; *Nat.Mater.*, **7**, 158 (2008).
- [8] Z.Xu, L.M.Chen, G.Yang, C.H.Huang, J.Hou, Y.Wu, G.Li, C.S.Hsu, Y.Yang; *Adv.Funct.Mater.*, **19**, 1 (2009).
- [9] J.Y.Kim, S.H.Kim, H.H.Lee, K.Lee, W.Ma, X.Gong, A.J.Heeger; *Adv.Mater.*, **18**, 572 (2006).
- [10] H.H.Liao, L.M.Chen, Z.Xu, G.Li, Y.Yang; *Appl.Phys.Lett.*, **92**, 173303 (2008).
- [11] C.Waldauf, P.Schilinsky, M.Perisutti, J.Hauch, C.J.Brabec; *Adv.Mater.*, **16**, 2084 (2003).
- [12] V.Shrotriya, G.Li, Y.Yao, T.Moriarty, K.Emery, Y.Yang; *Adv.Funct.Mater.*, **16**, 2016 (2006).
- [13] W.Ma, C.Yang, X.Gong, K.Lee, A.J.Heeger; *Adv.Funct.Mater.*, **15**, 1617 (2005).
- [14] G.Li, V.Shrotriya, Y.Yao, Y.Yang; *J.Appl.Phys.*, **98**, 043704 (2005).
- [15] X.Yang, J.Loos, S.C.Veenstra, W.J.H.Verhees, M.M.Vienk, J.M.Kroon, M.A.J.Michels, R.A.Janssen; *Nano.Lett.*, **5**, 579 (2005).
- [16] A.Swinnen, I.Haeldermans, P.Vanlaeke, J.Poortmans, M.D'Olieslaeger, J.V.Manca; *Eur.Phys.J.Appl.Phys.*, **36**, 251 (2007).